CNRS
Centre National de la Recherche Scientifique

INFN
Istituto Nazionale di Fisica Nucleare

AdV SLC: Characterization of Diamond-Like Carbon for coating baffles and beam dumps in AdV

VIR-0127A-13

Antonino Chiummo*, Benjamin Canuel, Andrea Magazzu, and Julien Marque

EGO - European Gravitational Observatory

Date: April 11, 2013

[*] *corresponding author:* antonino.chiummo@ego-gw.it

VIRGO* A joint CNRS-INFN Project - EGO* the site of the VIRGO project
Via E. Amaldi, I-56021 S. Stefano a Macerata - Cascina (Pisa)
Secretariat: Telephone (39) 050 752 521 * FAX (39) 050 752 550 * Email: ego@ego-gw.it

Contents

Introduction

In this document we report about the characterization of Diamond-Like Carbon (DLC) for application in gravitational-wave interferometric antennas as beam-dump of laser power at wavelength $\lambda = 1.064\mu m$ (Nd:YAG laser) [1]. A similar work was previously carried out by Takahashi *et al.* [2], in the framework of the now decommisioned Japanese interferometric antenna TAMA300 [3]. Further studies were carried out by [4, 5] to validate the use of this material both for ultra-high vacuum operations and as an effective absorber at YAG wavelength. Taking advantage of their early results, we decided to test DLC coatings on stainless steel 304 (X5CrNi18-10).
The deposition technique can alter significantly the properties, both mechanical and optical, of the layer. We took into account two kinds of deposition of the DLC onto the substrate, namely Physical Vapor Deposition (DLCpvd), and Chemical vapor deposition (DLCcvd).
Physical vapor deposition is a vacuum deposition method encompassing the condensation of a vaporized form of the desired film material onto various workpiece surfaces. The coating method involves purely physical processes such as high temperature vacuum evaporation with subsequent condensation, or plasma sputter bombardment. However, the resulting layer is not pure DLC, actually it is often made of Chrome + Tungsten + DLC, the DLC being the thinnest layer of the three. For instance, an $8\mu m$ thick film consists of just $1\mu m$-thick DLC layer. It shows good mechanical properties (e.g. adherence, wear resistance, etc.) but it fails in replicating the substrate surface roughness (non-conformal deposition).
Chemical vapor deposition (CVD) is a chemical process used to produce high-purity solid materials. The process is often used in the semiconductor industry to produce thin films. In a typical CVD process, the substrate is exposed to one or more volatile precursors, which react and/or decompose on the substrate surface to produce the desired deposit. This technique allows to deposit pure DLC, meaning that the whole thickness of the film is made of DLC. It is not easy to manufacture because it features less adherence than the DLCpvd, and it is more fragile, although very hard. Nevertheless, the resulting layer is *micro-conformal*, i.e. it reproduces the same micro-roughness as the substrate [6]. Of course this shifts the roughness requirements on the substrate surface. We bought plates of stainless-steel 304 with mirror finish surface (super #8) with nominal micro-roughness of $0.16\mu in$ or $4nm$ rms, provided by Mirrored Stainless Solutions LLC [7].

The tests we performed within the scope of the present work have been done upon some samples coated by *Poco Graphite* [8] with two different layer thicknesses, namely $1\mu m$ and $15\mu m$, of DLCcvd (commercial name "UltraC Diamond^{TM} Coating" [9]). We have as well characterized some samples of the bare substrate, the stainless-steel (SS) 304 plates.
In the following, we refer to the samples according to the ID-codes listed in annex A.

1 Cleaning of stainless-steel substrates

As said, the DLC deposited by plasma-enhanced chemical vapor deposition is, up to a point, *micro-conformal*, meaning that the layer replicates the substrate roughness. Therefore it is important to start from a substrate as clean and smooth as possible, before sending it for coating.
Unfortunately, when removing the protective plastic film from the stainless-steel plates we bought, we noticed some residuals on the otherwise mirror-like surface. Those residuals looked like glue or other organic material, but we do not have real hints about its nature as of the writing of this note.
After several attempts, we found that the best solvent to clean the stainless-steel substrates, as received from the vendor, was *Trichloroethylene*. We obtained best (but not perfect) results with the following procedure:

- blow clean air/inert gas on substrate to get rid of possible major debris on the surface;
- wipe gently the surface with soft anti-static rag;
- wipe gently the surface with soft anti-static rag moistened with isopropyl alcohol;
- wipe the surface with soft anti-static rag moistened with Trichloroethylene - repeat as needed.

The sample MSS_2 was cleaned with Trichloroethylene using the above procedure and tested before and after the cleaning. The pictures of figure 1 depict the same area of sample MSS_2, before (a) and after (b) cleaning.

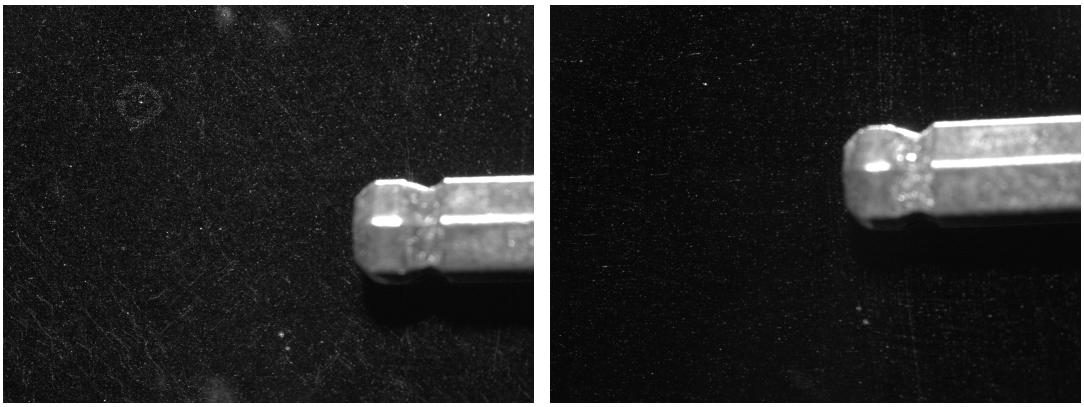

(a) (b)

Figure 1: Microscope pictures of bare substrate sample MSS_2 with same conditions of light, exposition time and zoom (the hex screwdriver is 2mm thick). (a): Before cleaning with the procedure described in the text. (b): After cleaning. It is evident that the density of defects is reduced by the cleaning, as confirmed by the scattering measurement.

They were taken with an optical microscope with the same light condition, and the same exposure time.
A visual inspection shows that the density of point defects is reduced, and also most of the larger defects are gone as an effect of the cleaning. So, cleaning with Trichloroethylene is effective in reducing the point defect density and also produces measurable results on the scattering from the sample (more on this later on). There are hints that also other kind of (larger) defects can be removed by means of this cleaning. Anyway, special care has to be payed while wiping the sample in order not to inflict scratches on the surface.

2 Refractive index, Reflectivity, and Absorption

In order to characterize the optical behavior of the DLC coating within the framework of SLC, we performed several measurements.
The measurement of the reflectivities for the two linear polarizations, as a function of the incident angle θ_{inc}, allows to derive the complex index of refraction and in turn both the Fresnel reflectivity and the absorption of the material. We measured the reflectivity at the YAG laser wavelength ($\lambda = 1064nm$) for S and P polarizations for the stainless steel substrate (sample MSS_1), a sample coated with a $15\mu m$-thick DLC layer (MD15_1) and a sample coated with just $1\mu m$m-thick DLC layer (MD1_1).
For opposite reasons, both MSS_1 and MD15_1 were supposed to give rise to reflections dictated by bare Fresnel's laws B.1, without taking into account any interference: MSS_1 had no coating and so just one dielectric interface to take into account, while MD15_1 had been coated with a $15\mu m$-thick layer of DLC, enough to absorb almost completely the field reflected off the substrate. On the contrary, due to the thinner DLC layer (thickness $d \sim \lambda$), reflection off MD1_1 had to be modeled by taking into account the reflectivity at the interface between DLC and Stainless Steel as well (see [2]). The resulting reflectivity is given by the Airy's sum of the fields coming from the two interfaces:

$$r_{s,p}(\theta_{inc}) = \frac{r_{1s,p}(\theta_{inc}) + r_{2s,p}\,(\theta_r)\ \exp\,(-2i\ \delta_1)}{1 + r_{1s,p}(\theta_{inc})\ r_{2s,p}\,(\theta_r)\ \exp\,(-2i\ \delta_1)} \tag{2.1}$$

where r stands for Fresnel's amplitude reflectivity (with subscripts 1 or 2 according to the interfaces air/DLC or DLC/metal, and s or p according to the polarizations), $\theta_r = \frac{n_0}{n_1}\ \arcsin\,(\theta_{inc})$ is the angle inside the DLC layer

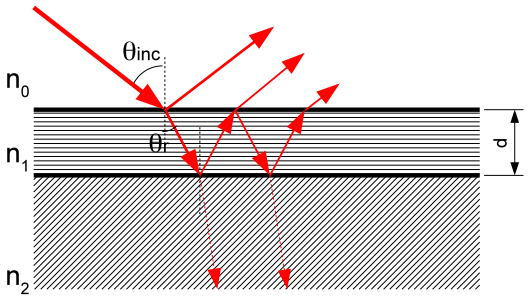

Figure 2: Sketch of the reflection process with two dielectric interfaces at a distance d. The light field comes from the medium with refractive index n_0 and impinges at an angle θ_{inc} onto the first interface. It is partially reflected (at the same angle) and refracted with an angle θ_r inside the medium with index n_1. Then it crosses a second interface between medium with indices n_1 and n_2. The fraction of the light that is reflected encounters again the interface between n_1 and n_0 before interfering (with a phase lag $2\delta_1 = 4\pi/\lambda\ n_1\ d\cos(\theta_r)$) with the light promptly reflected off the first interface.

(refractive index n_1), and $\delta_1 = 2\pi/\lambda\ n_1\ d\cos(\theta_r)$ half the additional phase experienced by the field traveling inside the layer, when compared with the field reflected off the interface air/DLC layer (see fig.2).

The outcomes of the measurements are reported in figure 3(a) for the substrate MSS_1, fig.3(b) for the sample MD1_1, and fig.3(c) for MD15_1. As expected, there is no visible interference occurring for the sample MD15_1. The measured reflectivity for $\theta_{inc} \sim 3° - 5°$ is of the order of 15% for MD15_1. This means that an AR coating is mandatory to use this material for SLC purposes. For the same sample, the *measured* Brewster's angle resulted to be $\tilde{\theta}_B \sim 67°$, giving an index of refraction $n_{DLC} = \tan(67°) = 2.35$, with a reflectivity of the order of 0.3%. However, in order to have consistent results for all the measurements, we used a Least Square algorithm to fit all the data with the respective functions at the same time, so to have a coherent estimation for all the meaningful parameters.
The adjustable parameters of the algorithm were the complex refractive index n_1 for DLC, the complex refractive index n_2 for the stainless steel substrate, the thickness d of the DLC layer for the sample MD1_1. From the best fit we have:

- $n_1 = 2.2$ - $0.05\imath$ DLC index of refraction
- $n_2 = 2.40$ -$4.6\imath$ SS index of refraction
- $d = 1.116\mu$m layer thickness for MD1_1

These results have to be compared with previous measurements [2] giving: n1 = 2.4 -$0.04\imath$; n2 = 2.5 -$4.1\imath$.

Although the fit outcomes look robust with respect to the variations of initial point and to slight modifications of the model, we consider safer an error bar on the imaginary part of about $\mathrm{Im}(n_1) = -0.05 \pm 0.01$. From this result, a lower limit can be given for the attenuation coefficient α_{DLC} of this kind of DLC at $\lambda = 1.064\mu m$:

$$\alpha_{DLC} = 4\pi\ \frac{|\mathrm{Im}(n_1)|}{\lambda} = 4.7\ 10^3 cm^{-1} \tag{2.2}$$

Let us consider the intensity I_t carried by the light that emerges from the DLC layer after having been reflected off the SS substrate, when a field with intensity I_0 is refracted at the interface between n_0 and n_1. The attenuation coefficient gives as residual relative intensity I_t/I_0 after a round trip in a 15um-thick layer: $I_t/I_0 = \exp(-\alpha_{DLC}\ 2d) = 0.7ppm$, so confirming the initial hypothesis that no interference occurs with such a thickness.

In table 2, we report the thickness of a DLC layer needed to obtain a given residual intensity after a round-trip. This table will be used to choose the actual thickness of DLC layers to be used to coat the baffles for AdV core optics. To summarize, a layer of 15μm of DLC provides more than enough absorption at YAG wavelength for SLC purposes (less than 1ppm of residual intensity after a round-trip). Nevertheless, AR coating is mandatory to use DLC for constructing the baffles for AdV, as primary Fresnel reflectivity is around 15% at $\theta_{inc} = 0°$.

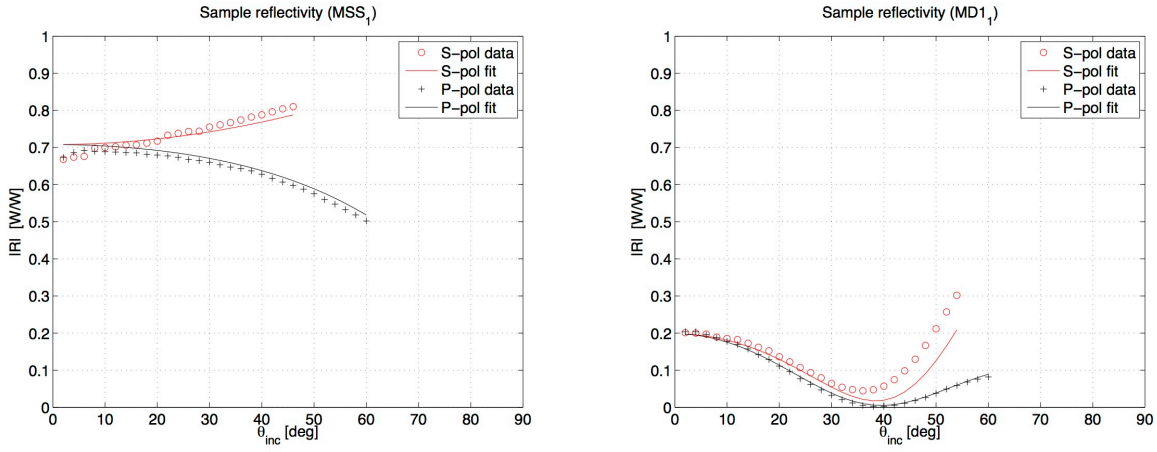

(a)

(b)

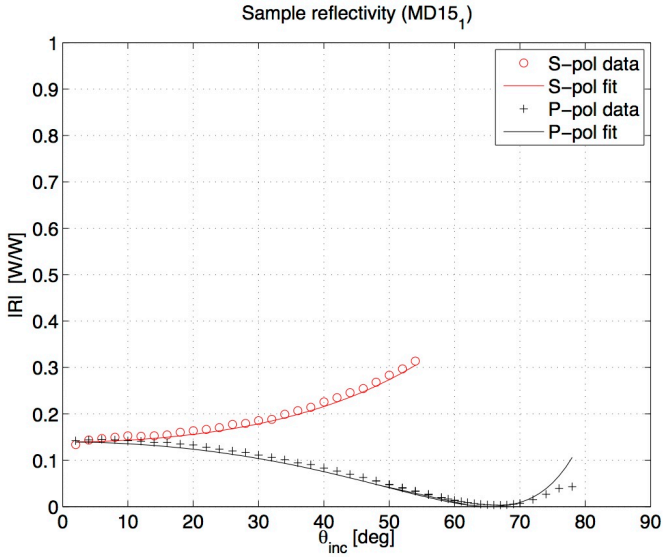

(c)

Figure 3: Measurements of (intensity) reflectivity as a function of the incidence angle θ_{inc} for three samples. (a): sample MSS_1, bare substrate. (b): sample MD1_1, 1μm-thick DLC layer. (c): sample MD15_1, 15μm-thick DLC layer. Red circles are the data for S-polarization, black crosses for P-polarization. The solid lines are the best-fitted theoretical model: red for S-polarization, and black for P-polarization. The parameters of the model have been drawn by best-fitting the whole data-set at the same time.

I_t/I_0 [ppm]	Thickness [μm]
1000	7.3
100	9.7
10	12.2
1	14.6

Table 1: DLC thickness needed to obtain a given residual relative intensity I_t/I_0 after that the light travels two times this thickness inside the layer. The worst-case extinction coefficient $\mathrm{Im}(n_1) = -0.04$ is assumed.

3 Scattering

3.1 Total Integrated Scattering (TIS) of samples

The Total Integrated Scattering (TIS) gives the fraction of the impinging power that is scattered towards various directions, and it is a parameter that should be as low as possible for SLC purposes. Under the hypothesis of perfect Lambertian scatterer, the TIS is linked to the bidirectional reflectance distribution function (BRDF) by [10]:

$$BRDF = \frac{TIS}{\pi} \tag{3.1}$$

We have measured the TIS for angles of incidence spanning $1^\circ < \theta_{inc} < 3^\circ$ for some of the coated samples and for the bare substrate, the results being reported in table 3.1. The setup and the technique were the same as used in [11] for the characterization of the SiC. We used an Integrating Sphere, with S-polarized YAG laser coming from the 0° port. The sample was put at the 90° port with respect to the incoming laser beam, other ports being closed with spectro-foam 100% scatterer caps. After measuring a reference P_{ref}, by closing all the ports but the input with the 100% scatterers, the TIS has been estimated by measuring the detected scattered power P_{scat} when the specular reflection from the sample is allowed to escape from the sphere:

$$TIS = P_{scat}/P_{ref} \tag{3.2}$$

The measurements were performed by scanning the sample position and by rotating the sample about the optical axis. If there were no huge differences between the measurements, only an average value is reported in table 3.1, otherwise a range is specified.
Along with the TIS, in table 3.1 we report also the effective μ-roughness rms, evaluated by:

$$rms = \frac{\lambda}{4\pi \ \cos(\theta_{inc})} \sqrt{TIS} \tag{3.3}$$

The effective rms for the bare substrates is well below the nominal μ-roughness as declared by the vendor, namely $0.16\mu in$ or $4nm$. From table 3.1, it is evident that there is a correlation between the DLC layer thickness and the

Sample	TIS [ppm]	rms [nm]
ED15_2	6181	6.7
ED15_1	5000 - 6500	6.3 - 6.8
ND15_1	6985	7.1
MD15_1	5402	6.2
MD15_2	6482	6.8
MD1_1	220 - 427	1.3 - 1.7
WD1_1	190 - 251	1.2 - 1.3
MSS_1	302	1.5
MSS_2(*)	390	1.7
MSS_2	208 - 256	1.2 -1.3
MSS_3	243	1.3

Table 2: Measured TIS at $\theta_{inc} \sim 2 - 3^\circ$ for the various samples, along with the effective roughness rms corresponding to measured TIS. The TIS for MSS_2 was measured two times: before cleaning (*), and after cleaning with trichloroethylene.

TIS value. While for the $1\mu m$-thick DLC the TIS is more or less the same as for the bare substrate, it increases by a factor 20 or more for the $15\mu m$-thick DLC. According to engineers of Poco Graphite [12], roughness of coated samples is known to be an increasing function (also) of the film thickness. This behavior is explained

with the presence of nodules of different density in the layer, whose size increases with the increase of the film thickness. The roughness is expected to be almost constant for coatings up to $5\mu m$, then this parameter increases with the film thickness.
We did not find third-party data on this topic as of the writing of the present note.
Based on those observations, SLC subsystem recommends to find a trade-off between the need of highest absorption (large thickness) and the need of low scattering (small thickness). A possible compromise is a coating with $7\mu m$-thick DLC layer, that would ensure 99.9% of absorption over a round trip (tab. 2) while keeping the μ-roughness of the surface almost at the substrate level.

3.2 Bidirectional Reflectance Distribution Function (BRDF) of samples

No measurement to report to date. Anyway some data are available from aLIGO [13], showing that the BRDF of DLC-coated stainless-steel substrates is as low as 3 10^{-5} sr^{-1} for angles of scattering $\theta_s \sim 5°$, and then reaches a plateau at around 3 10^{-7} sr^{-1} for $\theta_s > 15°$.

4 Surface cosmetics and microscope analysis

4.1 Edge sharpness

The edge sharpness is an important parameter for the baffles. If the radius of curvature (RoC) of the inner edge of the baffles is too long, then a relatively large surface is exposed to scattered light with a direction almost perpendicular to the impinging light. Rough calculations indicate that if the RoC is longer than $50\mu m$, then some problems could arise.
We had an external firm to cut samples of the substrate in different ways, namely using water-cutting, mechanical machining, or electrical discharge machining (EDM).
The best results were obtained by means of EDM. We examined the edge of samples ED15_1 and ED15_2 with an optical microscope, both cut by EDM. While ED15_2 underwent just one passage of the cutting procedure, ED15_1 was machined a second time too, in the attempt to improve roughness and sharpness.
Pictures 4(a) and 4(b) show the front view of the edge of ED15_2 and ED15_1 respectively (sample thickness is around 1.3mm). It is evident that the second passage of EDM reduced the roughness of the side face of the edges.

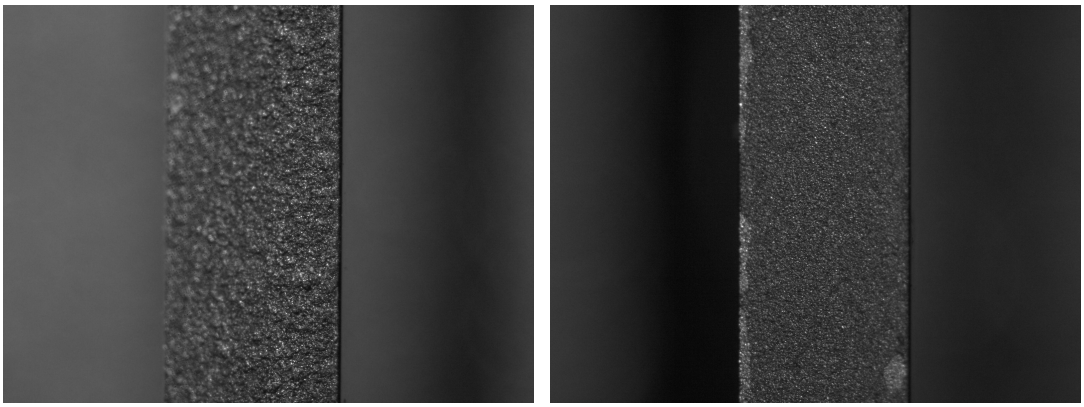

(a) (b)

Figure 4: EDM-cut samples, front view. (a): ED15_2 underwent just one passage of the cutting procedure. (b): ED15_1 was machined a second time too. It is evident that the second passage is effective in improving roughness and sharpness. The sample thickness is $\sim 1.3mm$ as a reference.

Pictures 5(a) and 5(b) show the same corner (EDM-cut edge is on the left) but for ED15_2 and ED15_1 respectively. From the pictures we can say that also the sharpness of the edge is improved by the second passage. A (very) rough estimation could be that RoC is less than $10\mu m$ for the edge of ED15_1 and a factor 2 (?) longer for ED15_2. Due to the large error bar of such a kind of visual estimation, the second passage with EDM is highly recommendable.
Furthermore, besides the shorter RoC, it seems that the DLC layer covers more uniformly the edge of ED15_1 than ED15_2's one.

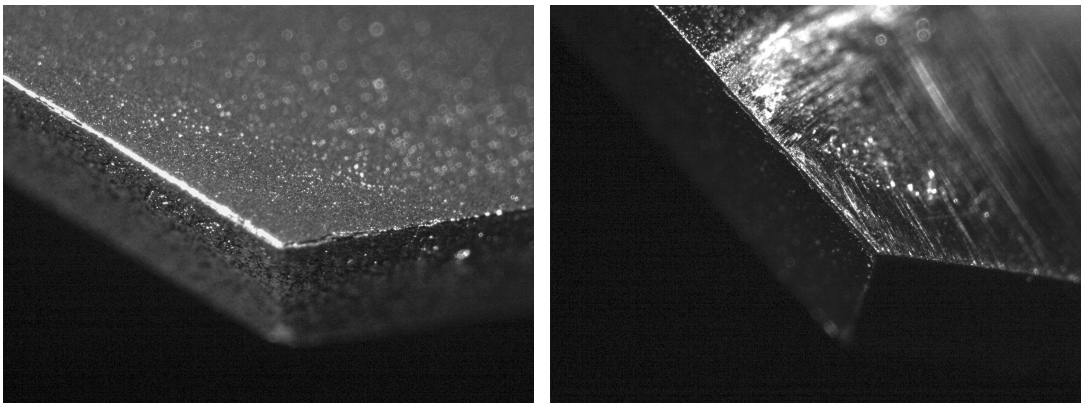

(a) (b)

Figure 5: EDM-cut samples, corner view. (a): ED15_2. (b): ED15_1. A (very) rough estimation could be that RoC is less than $10\mu m$ for the edge of ED15_1 and a factor 2 (?) longer for ED15_2. Furthermore, it seems that the DLC layer covers more uniformly the edge of ED15_1 than ED15_2's one. The sample thickness is $\sim 1.3mm$ as a reference.

4.2 Substrate surface cosmetics and scattering

The actual baffles will be made of stainless-steel substrate coated with DLC. But the substrate itself will undergo some machining to be conveniently shaped. This is a potential risk for the cosmetics of the surface for the substrate.
We had a first substrate plate machined to be used as Input Mode Cleaner baffle (IMCBaf), and analyzed its surface after proper cleaning (see pictures in fig. 6).

Picture 6(a) is the substrate (max diameter 320mm, as a reference) while fig. 6(b) is a close-up of scratches and other defects found on the surface of the sample after cleaning. From the pictures it is evident also that there is a problem of what seems to be residuals of glue or other organic material on the surface that was protected by a plastic film stuck to the sample.
Pictures 6(c), (d) refer to the surface of the sample, and were taken with the optical microscope. In fig. 6(c) the hex screwdriver is about 2mm, as a reference, and the field of view of figure (d) has the same size. Those pictures are a selection of the most striking defects found on the surface.
The effects of these defects has been evaluated by measuring the TIS of the substrate at small angle of incidence, following the usual procedure with some problems due to the size of the baffle substrate. The substrate was sampled in as many points as possible, and the largest scattering value was looked for at each location. Results of TIS measurement spanned the range 200ppm-1116ppm.
So the defects, although bad, do not seem to deteriorate the scattering of the substrate beyond acceptable level. SLC subsystem does recommend anyway to try to keep the cosmetics of the substrates as good as possible.

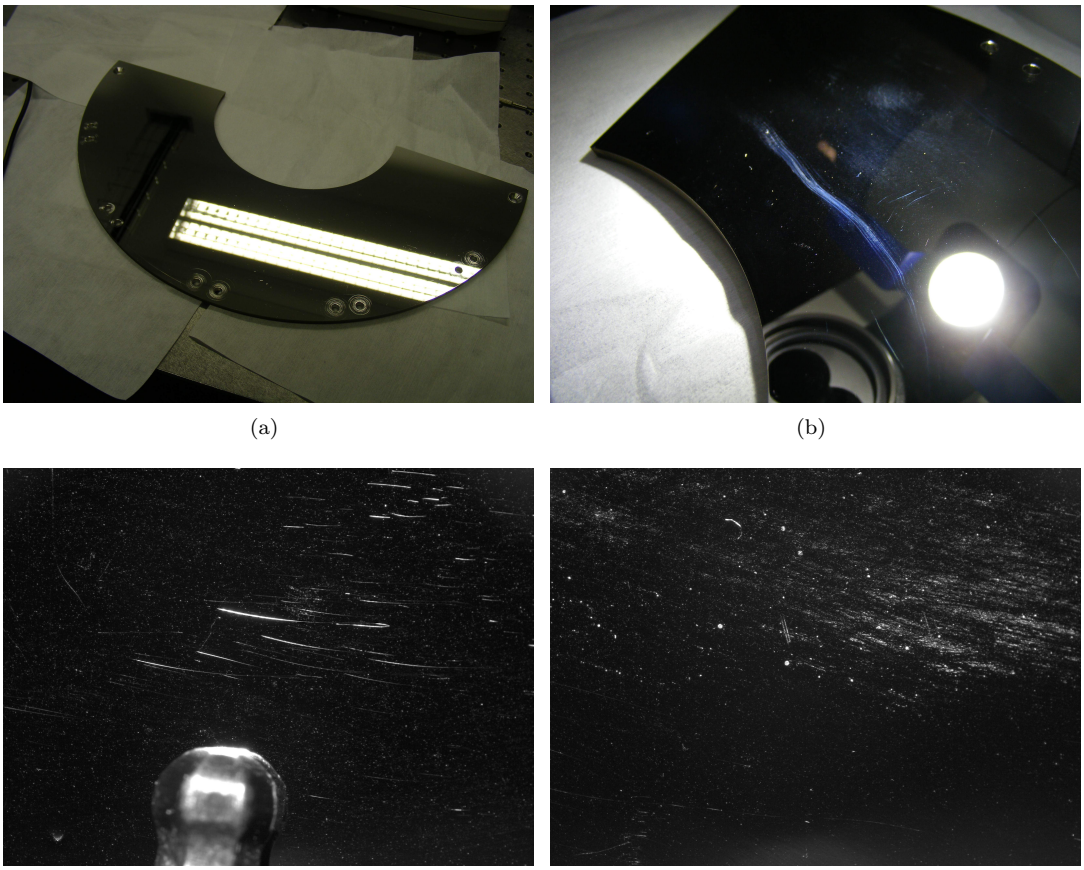

(a) (b)

(c) (d)

Figure 6: Pictures of the bare substrate for the IMC baffle. (a): The substrate after the cleaning procedure. Its maximum diameter is 320mm. (b): Close-up of an ugly scratch. The halo on the right of the scratch seems due to glue residuals, or some other organic materials, that we did not manage to get rid of. (c): Microscope picture of some scratches. The hex screwdriver is 2mm thick, as a reference. (d): Picture of other defects found on the substrate surface. The scale of the picture is the same as for fig. (c).

4.3 Coated samples surface cosmetics

After receiving the coated samples from the vendor, we took several pictures of each one both with the standard camera (macro) and with the microscope. The pictures were taken before attempting any cleaning.
Some of the samples have lighter spots with fuzzy borders with a diameter of some millimeters (see for instance 7(a)) This is probably due to the residuals on the substrates already mentioned before. Furthermore, the planarity of the samples does not look to be perfect (see for instance picture 7(b)), a possible cause being etching the ID codes on the back of the samples. In general, the surface of the coated parts looks significantly scratched, and there are many point defects of the order of 10-20μm (see picture 7(d) for an example, whole field=10mm). Other larger defects were noticed: see picture 7(c), same scale as fig. (d).
Despite all the defects noticed on the surfaces of the coated samples, we could not link any significant increase of their measured scattering to the defects themselves. Actually, as reported in table 3.1, the TIS of the coated samples was mainly due to the substrate roughness for the samples with 1μm-thick DLC layer, while the 15μm-thick coated samples feature a large TIS due to the increased roughness caused by the presence of nodules within the DLC layer (see sec. 3.1).
So we deem the present level of defects to be barely acceptable from the SLC point of view.

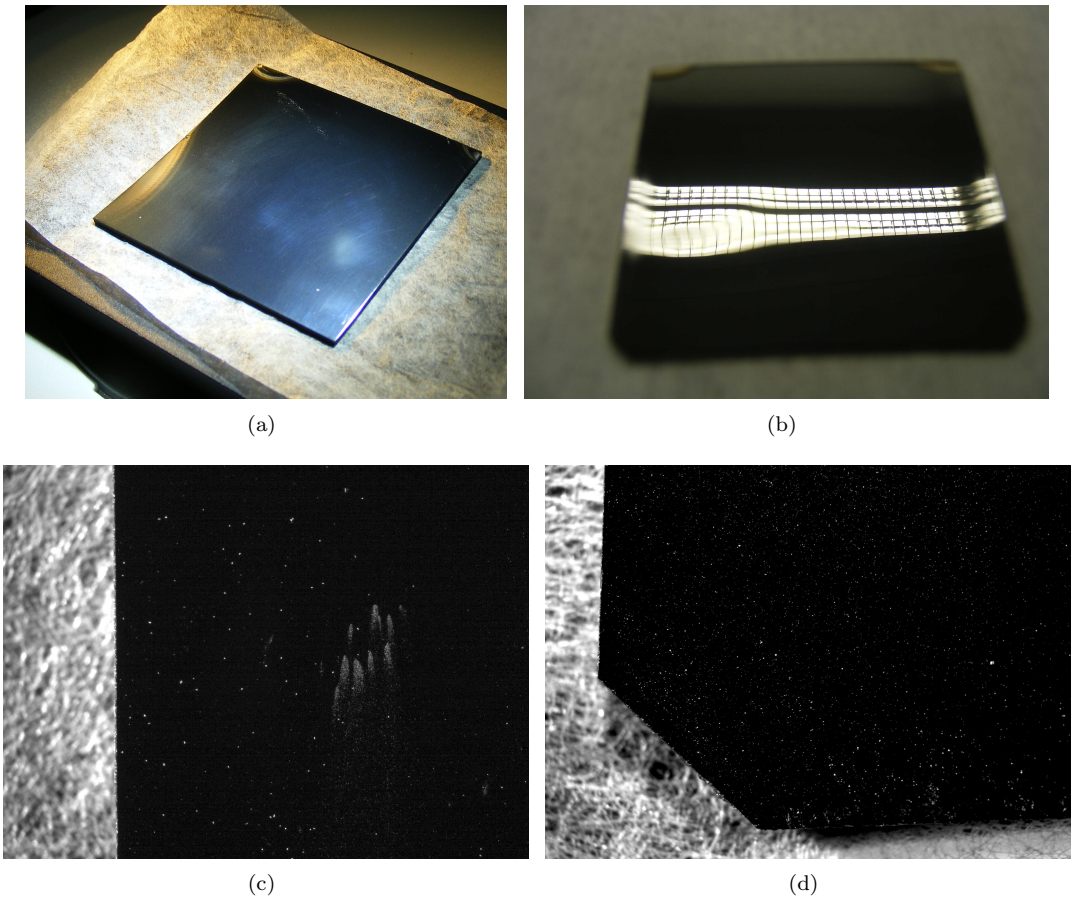

(a) (b)

(c) (d)

Figure 7: Pics of surface defects for coated samples. (a): Sample ND15_1 provides an example of light spots with fuzzy borders with a diameter of some millimeters (the side of the sample is 5 cm). They are probably due to organic material residuals on the substrate surface. (b): Sample ED15_2 shows that the planarity of the samples could be far from perfect. (c): Microscope image of sample MD1_1 (side of image $\sim 10mm$), showing defects of different size. (d): Sample MD15_1 with point defects of the order of 10-20μm.

4.4 Point defects

As mentioned in sec. 3.1, we noticed a correlation between the measured TIS (along with the effective roguhness rms) and the DLC layer thickness, and this correlation was confirmed by Engineers of Poco Graphite. Their experience is that the DLC coating replicates the substrate micro-roughness up to layer thickness of $\sim 5\mu m$. After this value, the roughness of the coated surface increases considerably with the thickness of the layer [12]. Indeed, also the amount of point defects observed by means of microscope analysis gave an indication along the same direction.
In figure 8, we report the pictures taken with the optical microscope for sample WD1_1 (1μm-thick DLC layer, fig. 8(a)) and sample MD15_2 (15μm-thick DLC layer, fig. 8(b)). Both the pictures were shot with the same light condition, zoom level, and exposure time, and no post-processing of images was performed. It is evident from the pictures that the quantity and density of point defects is much larger for the sample with the larger coating thickness.

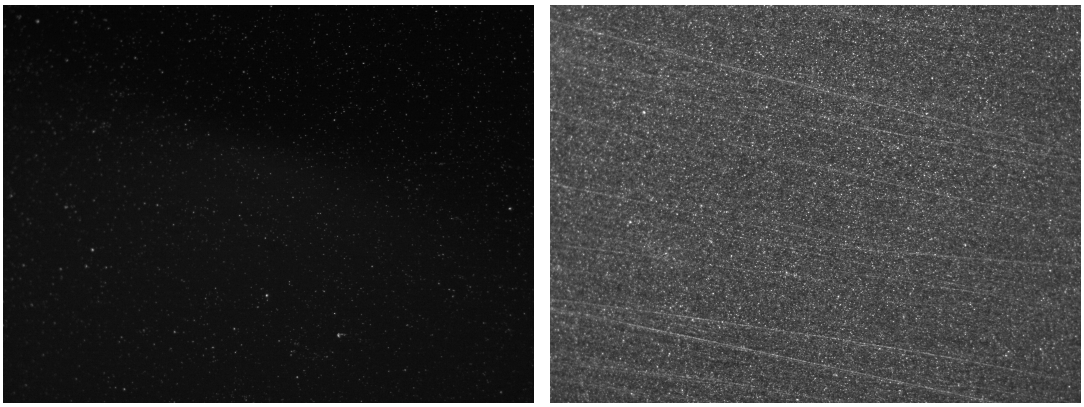

(a) (b)

Figure 8: Microscope pictures of two samples taken with same conditions. (a): WD1_1 is coated with $1\mu m$-thick DLC layer. (b): MD15_2 is coated with $15\mu m$-thick DLC layer.
A correlation is observed between number and density of point defects and DLC thickness.

5 Laser induced damage threshold

5.1 In-air damage threshold

We measured the damage thresholds for two samples from the Entegris DLC-coated set, namely MD15_1 and MD1_1. The setup consisted in an intense YAG laser beam focused onto the samples by a suitable telescope. The samples were put where the beam size was $w = 500\mu m$, then the power was slowly increased by means of a $\lambda/2$ - PBS cube combination, because the minimum set point for the Hi-Pow laser is about 9W, too intense for DLC. The measurement started by monitoring the surface of sample under test with a CCD camera, but the changes in diffusion were hardly noticeable, so we monitored instead the shape of the beam reflected off the sample, by using a simple IR viewer card.
With MD15_1, we noticed a rather sharp change in the reflected beam when the impinging power reached 4W (measured afterward). The shape of the beam changed from round to Laguerre-Gauss like (see picture 9(a)). Usually Laguerre-Gauss beams are originated when a TEM_{00} hits a phase mask with a phase singularity at the center, so the observed shape could be the sign that a damage had occurred on the sample surface at the center of the target area. Unfortunately, we were not able to identify this damage by means of the microscope (too many defects on the surface).
We repeated the same procedure with MD1_1. While monitoring the reflection, we noticed that in this case the change was far less abrupt. It started by causing a stronger and stronger focusing of the reflected beam and changed the shape to the already observed Laguerre-Gauss when the power was 4.7W (measured afterward). In this case we have a candidate for the occurred damage (although not perfectly sure), see picture 9(b).

To be noticed that in both cases the exposition to laser power lasted for less than one minute, so this could be regarded as a "transient" damage threshold.
Summarizing, the measured in-air "transient" (in the sense explained before) damage threshold I_{dmg}^{DLC} for DLC coating is of the order of:

$$I_{dmg}^{DLC} = \frac{I_0\ (1-R)}{\pi\ w^2} \sim 0.5 KW cm^{-2} \tag{5.1}$$

with R the (power) reflectivity at 0°.
No significant difference of values was noticed for the two thicknesses under test. As a comparison, we report here the laser induced damage threshold measured at EGO for two other interesting materials, Si (I_{dmg}^{Si}), SiC

(a) (b)

Figure 9: The laser induce damage threshold was measured for two samples coated with different DLC thickness. (a): The reflected beam from sample MD151_1 changed abruptly from a TEM00 to a Laguerre-Gauss. (b): A possible damage inflicted by the laser beam onto sample MD1_1.

(I_{dmg}^{SiC}) [14], and absorbing glass (I_{dmg}^{glass}):

$$I_{dmg}^{glass} = 1 W cm^{-2} \tag{5.2}$$

$$I_{dmg}^{Si} = 6 KW cm^{-2} \tag{5.3}$$

$$I_{dmg}^{SiC} = 30 KW cm^{-2} \tag{5.4}$$

5.2 In-vacuum damage threshold

No measurements to report to date.

6 Outgassing

Most of the baffles, beam dumps and diaphragms are intended to be put in ultra-high vacuum, so an important parameter to be measured is the outgassing rate of the material they are made of.
No measurements to report to date for DLC.
According to measurements carried out by [2], some samples coated by DLC film had an outgassing rate of less than 4 10^{-9} $Pa\ m^3\ s^{-1}\ m^{-2}$ at 50hr. In [4], this parameter was measured to be 9 10^{-9} $Pa\ m^3\ s^{-1}\ m^{-2}$ at 20 hours. While in [5], they managed to reach values for this parameter comparable with bare stainless steel: outgassing rate was measured to be less than 10^{-9} $Pa\ m^3\ s^{-1}\ m^{-2}$, after 140 hours of pumping including an 80 hour bake at 100 °C.
Although the outgassing rate is expected to be a function also of the deposition technique, the values reported in literature so far are encouraging for the compliance of DLC coating with ultra-high vacuum operations in large-scale gravitational-wave interferometric antennas.
As a reference, in [15] Stainless Steel 304 is an approved material for LIGO ultra-high vacuum operation and is reported to have a nominal outgassing rate (unbaked) of $\sim 2\ 10^{-5}\ Pa\ m^3\ s^{-1} m^{-2}$.

7 Electric conductivity

No measurements to report to date.

Aknowledgements

We wish to thank dott. Claudio Carini (LaFer) for useful discussions; M. Smail Aaziz and M. Hervé Benesville (Poco Graphite), Mr. Shane Collis (Entegris) for their cooperation. Furthermore, we wish to tank mr. Nicola Menzione (EGO) for useful discussions and help with the cleaning of the samples.

A Identity codes for the samples

(a) (b)

Figure 10: Stainless steel substrates before sending them to Entegris for coating. (a): Front, some of the samples underwent cleaning at EGO, some others were sent with the original protective film. (b): An identity code was etched on the back of the samples.

DLC coated samples:

- MD1_1: machine cut, DLC coating, $1\mu m$ thickness;
- WD1_1: water-jet cut, DLC coating, $1\mu m$ thickness;
- ED15_1: EDM cut, DLC coating, $15\mu m$ thickness;
- ED15_2: EDM cut, DLC coating, $15\mu m$ thickness;
- MD15_1: machine cut, DLC coating, $15\mu m$ thickness;
- MD15_2: (formerly "provino 4") machine cut, DLC coating, $15\mu m$ thickness;
- ND15_1: (formerly "provino 3") machine cut + electropolishing, DLC coating, $15\mu m$ thickness.

Uncoated stainless steel samples:

- MSS_1: stainless steel 304 substrate coupon cut in EGO workshop from a larger plate;
- MSS_2: stainless steel 304 substrate coupon cut in EGO workshop from a larger plate;
- MSS_3 stainless steel 304 substrate coupon cut with mechanical machines by an external firm;

All of the samples are pieces cut off from larger plates by Mirrored Stainless Solution LLC [7].

B Fresnel's equations

The amplitude reflectivity r for polarized light coming from a medium with refractive index n_0 at the interface with a medium with index n_1 is given by Fresnel's equations:

$$\begin{cases} r_s(\theta_{inc}) &= \dfrac{n_0\ \cos(\theta_{inc}) - n_1\ \sqrt{1-\left(\dfrac{n_0}{n_1}\ \sin(\theta_{inc})\right)^2}}{n_0\ \cos(\theta_{inc}) + n_1\ \sqrt{1-\left(\dfrac{n_0}{n_1}\ \sin(\theta_{inc})\right)^2}} \\ \\ r_p(\theta_{inc}) &= \dfrac{n_0\ \sqrt{1-\left(\dfrac{n_0}{n_1}\ \sin(\theta_{inc})\right)^2} - n_1\ \cos(\theta_{inc})}{n_0\ \sqrt{1-\left(\dfrac{n_0}{n_1}\ \sin(\theta_{inc})\right)^2} + n_1\ \cos(\theta_{inc})} \end{cases} \tag{B.1}$$

where θ_{inc} is the angle of incidence of the light impinging onto the dielectric interface and the subscripts $\{s, p\}$ stand for $s-$ and $p-$polarized light.

References

[1] The Virgo Collaboration, "Advanced Virgo Technical Design Report", 13 April, 2012 and updates; https://tds.ego-gw.it/ql/?c=8940

[2] R. Takahashi, Y. Saito, Y. Sato, T. Kubo, T. Tomaru, M. Tokunari, T. Sumiya, K. Takasugi, Y. Naito, "Application of diamond-like Carbon (DLC) coatings for gravitational wave detectors", Vacuum 73 (2004) 145-148.

[3] TAMA 300, a gravitational wave detector located at the Mitaka campus of the National Astronomical Observatory of Japan. http://en.wikipedia.org/wiki/TAMA_300

[4] T. Tomaru, et al. "Study of optical dumpers used in high vacuum system of interferometric gravitational wave detectors", 2006 J. Phys.: Conf. Ser. 32 476

[5] P.J.Kuzmenko, et al. "Hard, infrared black coating with very low outgassing", SPIE Advanced Optical and Mechanical Technologies in Telescopes and Instrumentation Marseille, France June 23, 2008 through June 28, 2008 LLNL-CONF-404403

[6] Private communication with dott. Claudio Carini, LaFer spa http://www.lafer.eu/lafer/index_en.php.

[7] Mirrored Stainless Solutions LLC; http://www.mirroredstainlesssolutions.com/

[8] Poco Graphite - an Entegris Company, http://www.poco.com/Applications/Coatings.aspx

[9] Entegris UltraC Diamond^{TM} Coating; http://www.entegris.com/Resources/Images/13571.pdf

[10] John C. Stover, "Optical Scattering: Measurement and Analysis", SPIE Press Monograph 1995

[11] A. Chiummo, B. Canuel, A. Magazzu, and J. Marque, "Characterization of Silicon Carbide for constructing baffles and beam dumps in AdV", Virgo internal note VIR-0460A-12 https://tds.ego-gw.it/ql/?c=9283

[12] Private communication with M. Smail Aaziz, Poco Graphite

[13] B. Swinkels, et al. "Report of the GW Detector Commissioning Workshop (2012 Cascina)", 2012/10/16 LIGO technical note LIGO-T1200464-v2, https://dcc.ligo.org/LIGO-T1200464-v2

[14] B.Canuel - "Damage threshold of SiC and Si" (Optics logbook 333) - https://pub3.ego-gw.it/itf/osl_hpio/index.php?callRep=333.

[15] D.Coyne, "LIGO Vacuum Compatible Materials List", LIGO technical note LIGO-E960050-v11